Journal of Statistical Physics, Vol. 117, Nos. 3/4, November 2004 (© 2004)

A Mixed-Transfer-Matrix Method for Simulating Normal Conductor/Perfect Insulator/Perfect Conductor Random Networks

Xiangting Li,[1,2] and David J. Bergman[1]

Received January 21, 2004; accepted April 5, 2004

We develop a mixed-transfer-matrix approach for computing the macroscopic conductivity of a three-constituent normal conductor/perfect insulator/perfect conductor random network. This is applied to two-dimensional and three-dimensional samples at a percolation threshold. Such networks are simulated in order to test whether a diluted percolating network of normal conducting bonds remains in the same universality class of critical behavior when a finite fraction of those bonds have been replaced by perfectly conducting bonds. Also tested by such simulations is whether a percolating mixture of normal and perfectly conducting bonds remains in the same universality class of critical behavior when a finite fraction of the normal bonds are replaced by perfectly insulating bonds. These questions are crucial for some recently published exact results which connect the macroscopic electrical and elastic responses of percolating networks.

KEY WORDS: Percolation; critical exponents; composite media; universality; elastic; electric.

1. INTRODUCTION

Interest in the critical behavior of macroscopic elastic stiffness moduli of percolating networks has been revived as a result of recent advances in the understanding of connections with the macroscopic electrical response of such networks[1,2]. In these references, an exact relation is argued to

[1]School of Physics and Astronomy, Raymond and Beverly Sackler Faculty of Exact Sciences, Tel Aviv University, Tel Aviv 69978, Israel; e-mail: bergman@post.tau.ac.il
[2]Institute of Theoretical Physics, Shanghai Jiaotong University, Shanghai 200240, People's Republic of China; e-mail: xiangtli@post.tau.ac.il

0022-4715/04/1100-0427/0

hold between the critical exponents t, T, which characterize how the macroscopic electrical conductivity σ_e and the macroscopic elastic stiffness moduli C_e tend to 0 when a randomly diluted network approaches its percolation threshold p_c from above:

$$\sigma_e \sim \Delta p^t, \quad C_e \sim \Delta p^T, \quad \Delta p \equiv p - p_c > 0, \quad T = t + 2\nu.$$

Here ν is the percolation correlation length critical exponent and p is the fraction of occupied or normal conducting bonds that are present in the diluted network, i.e., after the bonds marked for dilution have been removed.

Another exact relation, also argued to hold in those references, is that the critical exponents s, S, which characterize how σ_e and C_e tend to ∞ in a mixture of normal conducting or elastic bonds and perfectly conducting or perfectly rigid bonds when the fraction p of the latter bonds tends to p_c from below, are equal:

$$\sigma_e \sim |\Delta p|^{-s}, \quad C_e \sim |\Delta p|^{-S}, \quad \Delta p \equiv p - p_c < 0, \quad S = s.$$

It should be mentioned that, in order for the percolation threshold p_c to coincide with the elastic rigidity threshold, it is not enough that each bond has a bond stretching energy $k(\delta b)^2$, where δb is the change in length of the bond and k is the spring constant. It must also cost elastic energy to change the relative orientation of any nearest-neighbor bond pair, as well as the relative orientation of further-than-nearest-neighbor bond pairs, out to bond pairs that are separated from each other by a chain of $d-2$ intermediate bonds in the case of a d-dimensional network.[2,3] Such bond pairs are called "furthest neighbor bonds" and are denoted by FNB.

The arguments that $S = s$ and $T = t + 2\nu$, though quite rigorous, are based on some assumptions which, though reasonable, are unproven. These assumptions have to do with the ranges of universality of critical behavior in the relevant percolation problems.

One crucial assumption involves a diluted network, or a mixture of normal conducting or normal elastic bonds, denoted by M, and perfectly insulating or perfectly soft elastic bonds, denoted by I. Such a mixture is denoted by M/I. The assumption is that, if a finite fraction of the M bonds are replaced by perfectly conducting or perfectly rigid bonds, denoted by S, the critical behaviors of σ_e and C_e remain unchanged. i.e., the same values of t and T still characterize those behaviors. Such an altered network is made of three constituents, and is at or just above the

combined percolation threshold of the M and S bonds. We denote such networks by MS/I.

Another, similarly crucial assumption involves a two-constituent mixture of M and S bonds, which we denote by M/S. Here the crucial assumption is that, if a finite fraction of the M bonds are replaced by I bonds, the critical behaviors of σ_e and C_e again remain unchanged. i.e., the same values of s and S still characterize those behaviors. After this replacement, the network becomes a three-constituent network where the fraction of S bonds is still at or just below its percolation threshold. Such networks will be denoted by MI/S.

The two universality assumptions described above are required in order to argue that $S=s$ and $T=t+2\nu$ for networks with dimensionality d that is greater than 2[2]. Such assumptions usually cannot be justified rigorously, because the models in question are too complicated. Exact results vis-a-vis joint universality class for different models exist only for a few cases of solvable models that have a critical point, e.g., some of the two-dimensional Ising Hamiltonians.[4] Usually, universality properties can only be examined either by experiments or by approximate treatments of the models in question. In this article we attempt the latter approach.

It would seem, at first sight, that we need to do this separately for σ_e and for C_e of the altered networks. However, since the exact equalities $S=s$, $T=t+2\nu$ follow from the universality assumptions that we will be testing, it will actually suffice to verify those assumptions in the case of σ_e. The same conclusion regarding the critical behavior of C_e then follows automatically—see ref. 2. To this end, we develop a modification of the transfer matrix method for calculating the macroscopic conductance of a nonuniform, disordered resistor network. This modification is necessary in order to cope with the extreme situation of three-constituent mixtures of M, I, and S bonds. Such networks are denoted by $M/I/S$ in the general case. The notation MI/S is reserved for the special case of $M/I/S$ networks that are near the percolation threshold of the S constituent. Similarly, the notation MS/I is reserved for the special case of $M/I/S$ networks that are near the *joint percolation threshold* of the M and S constituents.

The rest of this article is organized as follows: Section 2 describes a new calculational approach, called "mixed-transfer-matrix method", which we have developed for simulating $M/I/S$ networks. Section 3 describes the results of simulations of MI/S and MS/I networks in two and three dimensions. Section 4 describes a more accurate test of universality using the same kinds of simulations. Finally, Section 5 summarizes our main conclusions and indicates avenues for further research. The appendices provide technical details connected with the calculational procedure described in Section 2.

2. CALCULATIONAL METHODS

2.1. Review of the Transfer Matrix Method

In the early 1980s, the transfer matrix method[5–7] was introduced for computing the conductivity of random networks made of either normal conducting and perfectly insulating bonds (M/I), or normal conducting and perfectly conducting bonds (M/S). A long strip $N_x \times N_y \times N_z$ ($N_x \times N_z$ in two dimensions (2D)) was constructed by adding bond after bond, gradually building up the strip along the x-direction. In the M/I case (see Fig. 1(a)), all the sites at $n_z = 1$ and $n_z = N_z + 1$ are connected by perfectly conducting bonds, i.e., the strip was put between two equipotential plates, like those of a parallel plate capacitor. For a three-dimensional (3D) strip, a periodic boundary condition was imposed along the y-direction. Voltages V_i ($i = 1, \ldots, m$; $m = N_y \times (N_z - 1) + 2$ in 3D, $m = N_z + 1$ in 2D) were applied to each of m external sites, called "terminal sites (TS)", at the edge of the strip under construction in the x-direction, resulting in currents I_j that flow into the TS j. The macroscopic current flows across the strip along the z-direction. The relation between the voltages and currents at

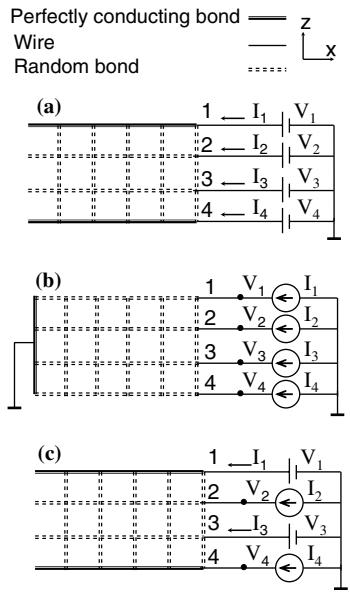

Fig. 1. (a) Two-dimensional strip of M/I, $N_z = 3, m = 4$. (b) Two-dimensional strip of M/S, $N_z = 4, m = 4$. At $n_x = 0$, the voltage is 0. (c) Two-dimensional strip of $M/I/S$, $N_z = 3, m = 4$. A zero-current boundary condition is applied at all the $n_x = 0$ sites. $A = [V_1, I_2, V_3, I_4]^t$, $B = [I_1, V_2, I_3, V_4]^t$, $\Theta = [1, -1, 1, -1]$.

the TS is given by the conductance matrix G

$$I = GV,$$

where $I = [I_1, I_2, \ldots, I_m]^t$, $V = [V_1, V_2, \ldots, V_m]^t$. At the end of the strip, an entire layer of insulating bonds is added. This makes all the elements of G vanish with the exception of G_{11}, G_{mm}, G_{1m}, and G_{m1}. In particular, G_{11} relates the voltage applied between the lower ($n_z = N_z + 1$) and upper ($n_z = 1$) surfaces to the total current flowing between those surfaces. If the length of the strip is N_x, then the conductance Σ per unit length of the strip is given by

$$\Sigma = \lim_{N_x \to \infty} G_{11}/N_x.$$

In the case of M/S (see Fig. 1(b)), currents $I_i (i = 1, \ldots, m)$ are applied to each of m ($m = N_y \times N_z$ in 3D, $m = N_z$ in 2D) TS, while periodic boundary conditions are applied in the y- and z-directions. The voltages and currents are now related by the resistance matrix R:

$$V = RI.$$

The first layer of the strip ($n_x = 0$) is now taken to be an equipotential plate by starting the calculation with $R \equiv 0$. At the end of the strip ($n_x = N_x + 1$), an entire layer of perfectly conducting bonds is added, resulting in another equipotential plate. The inverse conductance per unit length of the strip is then given by

$$\Sigma^{-1} = \lim_{N_x \to \infty} R_{ii}/N_x, \quad i = 1, \ldots, m,$$

where i can have any value.

The main reason for using the transfer matrix method for simulations of disordered conducting networks is numerical efficiency: while direct solution of Kirchhoff's equations (by Gaussian elimination or other efficient method) requires $\mathcal{O}(n^3) = \mathcal{O}(N^{3d})$ operations, where $n = N^d$ is the total number of network sites in a d-dimensional hypercubic sample network, the transfer matrix method only requires $\mathcal{O}(N^{3d-2})$ operations. Moreover, the appearance of many isolated TS (i.e., a TS that is not electrically connected to any other TS) in an M/I network close to its percolation threshold considerably reduces the number of nontrivial operations needed in the computations.[7] Similarly, the appearance of many perfectly

connected pairs of TS (i.e., a pair of TS that are connected to each other by a path of perfectly conducting bonds) in an M/S network close to its percolation threshold also reduces the number of nontrivial operations considerably.

The reason why different approaches are necessary in the implementation of the transfer matrix method to M/I and M/S networks has to do with the possible appearance of infinite values for some of the elements of the matrices R and G: R will have such an element $R_{ij}=\infty$ whenever the TS i and j happen to be electrically unconnected. Similarly, G will have an infinite element $G_{ij}=\infty$ whenever the TS i and j are connected by a path of perfectly conducting bonds. Clearly, when trying to implement the transfer matrix method for a three-constituent $M/I/S$ network, neither of the above approaches is acceptable: both matrices R and G will sometimes have infinite elements during intermediate stages of the simulation, even when the final macroscopic conductance and resistance of the completed sample are finite. This problem cannot be easily overcome by the trivial solution of replacing ∞ by a very large finite constant, and replacing $1/\infty$ by 0: in the calculations we would sometimes wind up with different large constants that represent ∞, and these would sometimes lead to erroneous results when these large constants do not properly cancel each other out. Also, suppose that an infinite conductance path connects between two TS, say i and j. If a third TS, denoted by 1, is connected to i and j by finite conductance paths, then although $G_{ii}=G_{jj}=G_{ij}=G_{ji}=\infty$, the values of G_{1i}, G_{i1}, G_{1j}, G_{j1} are not uniquely defined: if all the TS voltages are 0 except for V_1, then a definitely determined current $I_1=G_{11}V_1$ will flow into TS 1, but part of this same current can flow out of the two TS i and j in different proportions which are *indeterminate*.

In order to deal more effectively with the simulation of $M/I/S$ networks, we therefore introduce below a "mixed-transfer-matrix" method. In this approach, each TS of the network can have either a voltage or a current applied to it, and there is a resulting current or voltage at each of those TS. This scheme is the discrete analogue of a mixed boundary condition in a continuum system, where on parts of the boundary the electric potential is specified, while on other parts it is the normal current density that is specified.

2.2. The Mixed-Transfer-Matrix Method

In the simulation of three-dimensional (3D) networks, we use a simple cubic lattice, while the square lattice was used for simulation of two-dimensional (2D) networks. The boundary conditions in the z- and y-directions are the same as in the M/I case, namely equipotential plates

at $n_z = 1$ and $n_z = N + 1$, and periodic boundary conditions along y in the 3D case. In the x-direction, a zero current boundary condition is applied at all the final TS, i.e., at the end of the calculation. The fractions of I, M, and S are denoted by p_I, p_M, and p_S, respectively. The strip is constructed by adding bond after bond with conductance chosen randomly to be either 0, 1, or ∞ with the appropriate probabilities. Fig. 1(c) shows such a 2D strip under construction. Bonds that lie along the x-direction are called x-bonds, and similarly y-bonds and z-bonds. In order to measure the electrical properties of the completed part of the strip, voltages V_i or currents I_i are applied at each of the TS i, resulting in a current I_j or a voltage V_j at each TS j. The strip is built up along the x-direction. Adding a y-bond or a z-bond does not change any of the TS. By contrast, adding an x-bond changes one TS into an internal site, which can be omitted from subsequent considerations, but adds a new TS at the dangling end of that bond. The new TS replaces the discarded one in subsequent considerations. Thus the total number of TS remains constant throughout the calculation, even though the strip length keeps increasing. The number of TS is m, where $m = N_z + 1$ in 2D strips and $m = N_y \times (N_z - 1) + 2$ in 3D strips. We define mixed vectors A and B: The elements of A and B are voltages or currents at the various TS. Two elements at the same position in A and B are always of different character: If A_i is voltage, then B_i is current, and vice versa. A represents voltages and currents that are imposed, B represents resulting quantities. Because the problem is linear, A and B are connected by a matrix D

$$B = DA. \tag{1}$$

As a consequence of this definition, the physical dimensions of some elements of D are Ohm·m, others are $(\text{Ohm}\cdot\text{m})^{-1}$, and yet others are dimensionless—D is a mixed matrix. We use a characteristic vector $\Theta = \{\theta_1, \theta_2, \ldots, \theta_m\}$, with elements that are ± 1, in order to indicate the physical character of the elements of A and B:

$$\begin{aligned} \theta_i = 1 &\Leftrightarrow A_i = V_i, \qquad B_i = I_i, \\ \theta_i = -1 &\Leftrightarrow A_i = I_i, \qquad B_i = V_i. \end{aligned} \tag{2}$$

For each bond that is added, D and Θ must be updated. Changing Θ is necessary in order to prevent the appearance of infinite elements in the matrix D. An appropriate Θ ensures that all the elements of D are noninfinite. Taking into account all the different possible cases, there are five different procedures for adding an x-bond and seven different procedures for adding a y-bond or z-bond. Some of these procedures are quite

complicated, therefore their description is relegated to Appendix D. Some general properties of D are described in Appendices A and B—those properties are useful in computations.

The sizes of strips in our calculation are $N_x \times N_z$ and $N_x \times N_y \times N_z$ for 2D and 3D networks. The zero currents boundary condition at the beginning ($n_x = 0$) and end ($n_x = N_x + 1$) of the strip is imposed as follows: we start the simulation with $D_{ij} = 0$, $\theta_i = 1$ ($i, j = 1, \ldots, m$), and end it by adding a last layer ($n_x = N_x + 1$) of x-bonds that are all perfectly insulating except for the TS which represents the top equipotential plate ($n_z = 1$) and the TS which represents the bottom equipotential plate ($n_z = N_z + 1$). Thus, all the elements of D will vanish except for D_{11}, D_{1m}, D_{m1}, D_{mm}, while all the elements of Θ equal 1 with the possible exception of θ_m. We keep $\theta_1 = 1$ throughout the calculation, therefore, if $\theta_m = 1$ too, then the conductance of the strip is given by D_{11}. However, if $\theta_m = -1$, then the TS 1 and m must be connected by a path of perfectly conducting (S) bonds (see Appendix C). Consequently, the macroscopic conductance is then infinite. In this case the only nonzero elements of D are $D_{m1} = -D_{1m} = 1$.

In an $M/I/S$ strip with a non-negligible value of p_S, if the length N_x is much greater than the widths N_z, N_y, then the probability of having an S path which connects the equipotential plates at $n_z = 1$ and $n_z = N_z + 1$ approaches 1. For that reason we only simulated long strips for small values of p_S. Most of our simulations were of short strips, constructed at the percolation threshold of the constituent with the largest conductivity, where all the two or three linear sizes N_x, N_y, N_z were equal to N, and N went up to 30 in 2D samples, up to 12, or sometimes even 15, in 3D samples. In such systems, the macroscopic response does not saturate or "self average" with increasing N—the sample-to-sample fluctuations remain large even when N is very large. We therefore had to simulate a large number of samples at each value of N, and then compute the ensemble average, standard deviation, standard error, etc. For small values of p_S, we also simulated a small number of very long 3D strips, with $N_x \gg N_z, N_y$, where σ_e remained finite, in order to compare with the ensemble averaged σ_e from the short strips. The results of these two types of simulations were consistent, as will be shown below.

3. RESULTS OF NUMERICAL SIMULATIONS

Three kinds of macroscopic conductivities are possible in $M/I/S$ systems: 0 (the strip is perfectly insulating or I, the total number of such strips is denoted by N_I), ∞ (the strip is perfectly conducting or S, the total number such strips is denoted by N_S), finite (their number is denoted by N_M). σ_n denotes the finite conductivity of the short strip n. The

fraction of S strips in MS/I networks and that of I strips in MI/S networks is less than 0.01 when p_S in MS/I and p_I in MI/S are less than 0.12. Therefore these networks, for which the macroscopic conductivity or resistivity, respectively, diverges, are ignored in the statistical analysis described below. For each size of networks, we simulated 10,000 short strips in 3D and 50,000 in 2D. The average macroscopic conductivity σ_e for MS/I is given by

$$\sigma_e = \frac{1}{N_M + N_I} \sum_{n=1}^{N_M} \sigma_n, \tag{3}$$

while for MI/S it is given by

$$\frac{1}{\sigma_e} = \frac{1}{N_M + N_S} \sum_{n=1}^{N_M} \frac{1}{\sigma_n}. \tag{4}$$

The last expression is just the arithmetic mean of the resistivities of the various samples. The statistical error of each of these average values was always estimated by calculating the standard error. In order to aid the reader in visualizing the distribution of values of the conductivity for short strip samples of a particular size, prepared at the percolation threshold, we show such a distribution in Fig. 2 for the case of 3D normal conducting short strips of MS/I networks.

We have carried out calculations of the conductivity for strips of various sizes in the vicinity of the percolation threshold for 2D and 3D versions of the two kinds of random networks. The results for MS/I of 2D random networks with $p_S = 0.06$ and various values of p_I in the neighborhood of 0.5 are displayed in Fig. 3. One can see how the behavior of the conductivity as a function of strip size N changes when p_I is varied around 0.5. Clearly, $p_c = 0.50$ is still the critical point even when 6% of S bonds are present, replacing the same amount of M bonds. Similar results are obtained for the other three cases—MI/S in 2D, MS/I and MI/S in 3D. We therefore assume, in all further calculations, that the conductivity threshold has the same value as the percolation threshold in the case of simple M/I or M/S networks. An ensemble of samples are simulated, all of which are at that threshold, and the finite size scaling hypothesis[4] is used to compute the critical exponents t/ν and s/ν.

Fig. 4 shows log-log plots of σ_e vs. $N \equiv N_z = N_x$ at p_c, for different fractions p_S of the S bonds which replace M bonds in a 2D MS/I network with $p_I = 1 - p_c = 0.5$. From the slopes of these plots, the values of

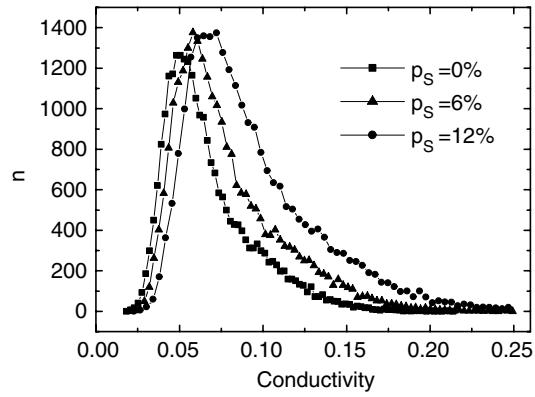

Fig. 2. Abundance (i.e., number of samples) n vs. conductivity for an ensemble of short strip, 3D, MS/I networks at the percolation threshold, i.e., when $p_I = 1 - p_c$, where $p_c = 0.2492$. The values of the fraction p_S of perfectly conducting bonds in the three-constituent random network are indicated in the figure. The fraction of normal bonds in each case is given by $p_M = p_c - p_S$.

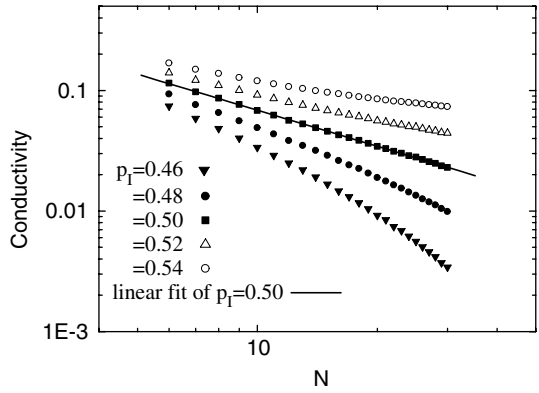

Fig. 3. Log-log plot of the conductivity of short 2D MS/I random strips vs. strip size N, in the vicinity of the percolation threshold $p_c = 0.5$. The fraction p_S of S bonds was always 0.06.

t/ν immediately follow. A least-squares fit gives

$$t/\nu = 0.987 \pm 0.018, \qquad p_S = 0.0,$$
$$t/\nu = 0.990 \pm 0.018, \qquad p_S = 0.06,$$
$$t/\nu = 0.995 \pm 0.020, \qquad p_S = 0.12.$$

A similar procedure, applied to 3D MS/I networks with different values of p_S, leads to Fig. 5, where σ_e is plotted vs. $N \equiv N_z = N_x = N_y$ for

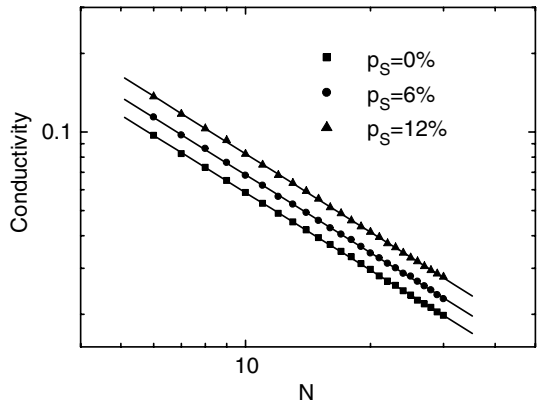

Fig. 4. Log-log plot of conductivities of 2D MS/I short random networks vs. the strip size N, at $p_M + p_S = p_c = 0.5$ but with different values of the fraction p_S of perfectly conducting bonds. Straight lines are linear fits.

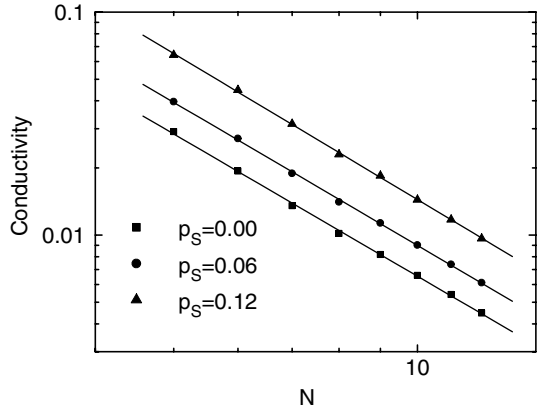

Fig. 5. Log-log plot of conductivities of 3D MS/I short random networks vs. the strip size N, at $p_M + p_S = p_c = 0.2492$ but with different values of the fraction p_S. Straight lines are linear fits.

$p_I = 1 - p_c \cong 0.7508$ and different fractions p_S of the S bonds. From the slopes of these plots, the values of t/ν are found to be

$$
\begin{aligned}
t/\nu &= 2.16 \pm 0.05, \qquad & p_S &= 0.0, \\
t/\nu &= 2.23 \pm 0.05, \qquad & p_S &= 0.06, \\
t/\nu &= 2.28 \pm 0.05, \qquad & p_S &= 0.12.
\end{aligned}
$$

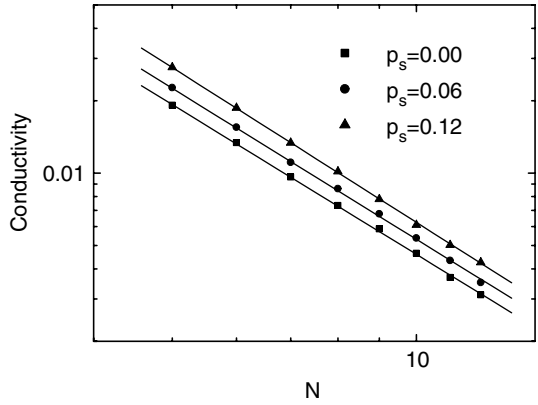

Fig. 6. Log-log plot of conductivities of 3D MS/I long random networks with $N_x = 50{,}000$ vs. the lateral strip size $N \equiv N_z = N_y$, at $p_M + p_S = p_c = 0.2492$ but with different values of the fraction p_S. Straight lines are linear fits.

We also simulated some long strips of 3D MS/I networks with the same values of p_I and p_S, in order to compare with the above results. These strips had $N_x = 50,000 \gg N \equiv N_z = N_y$, and lead to the plots shown in Fig. 6. The resulting values for the critical exponent are

$$\begin{aligned} t/\nu &= 2.08 \pm 0.04, \qquad p_S = 0.0, \\ t/\nu &= 2.11 \pm 0.05, \qquad p_S = 0.06, \\ t/\nu &= 2.19 \pm 0.03, \qquad p_S = 0.12. \end{aligned}$$

These differ slightly from the previous three values, and also show a slight systematic trend with changes in p_S. The other kind of 3D three-constituent network, namely MI/S, could not be simulated as long strips using the same algorithm, because the long equipotential plates at $z = 1$ and $z = N_z + 1$ are always connected by some perfectly conducting paths when the length N_x is large enough. We also found that long strip samples of 2D three-constituent networks were untreatable because, even in the case of MS/I strips, some perfectly conducting paths appeared in the sample even at low concentrations of the S constituent. That is why we have long strip results only for the case of 3D MS/I networks.

Figure. 7 shows plots of σ_e vs. N at p_c, for different fractions p_I of the I bonds which replace M bonds in a 3D MI/S network where $p_S = p_c \cong 0.2492$. From the slopes we get the following results for the critical

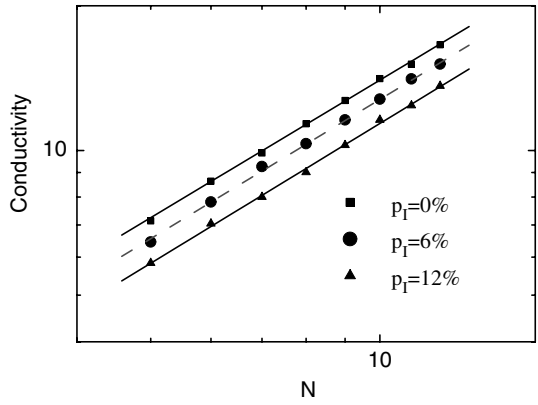

Fig. 7. Log-log plot of the conductivities of 3D MI/S short random networks vs. the strip size N, at $p_S = p_c = 0.2492$ and different fractions p_I of I bonds. Straight lines are linear fits.

exponent s/ν

$$s/\nu = 0.95 \pm 0.04, \qquad p_I = 0.0,$$
$$s/\nu = 0.96 \pm 0.04, \qquad p_I = 0.06,$$
$$s/\nu = 0.96 \pm 0.04, \qquad p_I = 0.12.$$

A similar procedure, applied to 2D MI/S networks, leads to Fig. 8 and to

$$s/\nu = 0.96 \pm 0.02, \qquad p_I = 0.0,$$
$$s/\nu = 0.97 \pm 0.02, \qquad p_I = 0.06,$$
$$s/\nu = 0.98 \pm 0.02, \qquad p_I = 0.12.$$

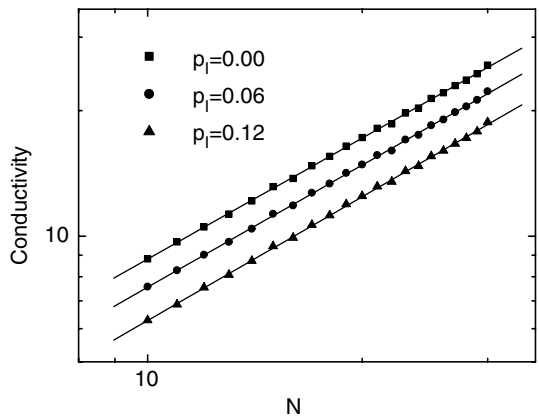

Fig. 8. Log-log plot of the conductivities of 2D MI/S short random networks vs. the strip size N, at $p_S = p_c = 0.5$ and different fractions p_I. Straight lines are linear fits.

The data presented above is consistent with the idea that the critical exponents do not change when a finite fraction of M bonds are replaced by S bonds in the case of M/I, or by I bonds in case of M/S. Nevertheless, the error bars on these results are somewhat larger than those found in earlier calculations, which were performed on simple two-constituent percolating networks[5–7]. Moreover, there is a slight systematic variation of the values found for t/ν with increasing p_S, as well as a slight systematic variation of the values found for s/ν with increasing p_I. A reviewer has suggested that these errors might be reduced, in the 3D case, if we used a different value for p_c in that case, namely $p_c = 0.2488$,[4] instead of $p_c = 0.2492$ which was used in our calculations. In order to alleviate all of these problems, we resorted to an alternative procedure for analyzing the simulation results. This is explained in Section 4 below.

4. HIGHER ACCURACY TEST OF UNIVERSALITY

The results described in Section 3 lend support to the idea that M/I and MS/I networks are in the same universality class of critical behavior, as are also the M/S and MI/S networks. Nevertheless, it would be desirable to have a stronger result: the large sample-to-sample fluctuations in the macroscopic conductivity of short strips means that, even with the rather large statistics which we amassed, the error bars are still quite large. Even more troubling are the apparent systematic changes in the computed critical exponents as p_S increases in the MS/I mixtures and as p_I increases in the MI/S mixtures. Large systematic errors are expected to occur due to the small values of N that were used in our simulations, namely, $N \leq 30$ in 3D and $N \leq 15$ in 3D. For such small values of N, non-negligible corrections to the asymptotic critical behavior can be expected. In the 3D case, the absence of duality symmetry brings about a dependence on N of p_c itself. This, along with a possible error in the asymptotic value of p_c for $N \to \infty$, can also contribute to the systematic error when finite size scaling is applied to simulations on finite size samples at p_c.[4]

In order to circumvent, or at least lessen, some of these errors, we applied an approach that was first used in the past to test whether the electrical conductivity and elastic stiffness moduli of an M/S network diverge with the same exponent at P_c.[8]

The basic idea in ref. 8 was to compare the two properties (electrical conductivity and elastic stiffness) on *identical or strongly correlated network samples*, before computing any ensemble averages. In the present case, the same idea is implemented by simulating strongly correlated pairs of networks: we first simulate a randomly constructed M/I sample network and compute its macroscopic conductivity $\sigma_e(p_S = 0)$. we then

randomly reset a fraction $p_S/(1-p_I)$ of the M bonds *in that same sample* to be S bonds, thus changing it into an MS/I sample network, and recalculate $\sigma_e(p_S \neq 0)$. We then compute the ratio of these two macroscopic conductivities

$$R_S \equiv \frac{\sigma_e(p_S \neq 0)}{\sigma_e(p_S = 0)}.$$

After repeating this for many such correlated network pairs of linear size N, we calculate ensemble averages and standard deviations of the ratio R_S. In principle, these values should depend on N and p_S. Our first expectation is that the actual deviations of σ_e, systematic as well as random, from its ensemble average value, will be similar for the two samples in every correlated pair of M/I and MS/I samples. Therefore the ratio R_S should exhibit reduced random fluctuations, as well as smaller systematic deviations from the simple asymptotic dependence on the linear size N. In fact, because we are trying to verify the hypothesis that the M/I and MS/I networks exhibit the same kind of critical behavior, we hope to find that $R_S(N, p_S)$ is in fact independent of N for any fixed value of p_S, but keeps changing with p_S.

Similar considerations can be applied to correlated pairs of M/S and MI/S sample networks, where the MI/S sample is obtained from the M/S sample by randomly resetting a fraction $p_I/(1-p_S)$ of the M bonds to be I bonds. The ratio

$$R_I \equiv \frac{\sigma_e(p_I \neq 0)}{\sigma_e(p_I = 0)}$$

is again calculated for many such pairs, and then analyzed statistically. The ensemble average and standard deviation will depend on N and p_I, in principle. However, if the M/S and MI/S networks belong to the same universality class of critical behavior, then $R_I(N, p_I)$ should be independent of N for any value of p_I. Again, the random sample-to-sample fluctuations of σ_e, as well as the systematic N-dependent deviations from simple asymptotic scaling, should partially cancel out in the computation of R_I.

In performing this kind of analysis, we discard all samples that have either zero or infinite macroscopic conductivity. Therefore, even though we always simulated a fixed number (10,000) of samples, the number N_M which were analyzed fluctuated somewhat from case to case. Nevertheless, that number was usually between 4000 and 5000.

The results for $R_I(N, p_I)$ and $R_S(N, p_S)$ were analyzed in two fashions: (a) The arithmetic average over all samples with given values of N, p_I or N, p_S were calculated and are plotted vs. N in Figs. 9–12.

Clearly, the points lie, approximately, on horizontal straight lines. These points were least-squares fitted to straight lines $aN+b$. The values for a and b, along with standard errors, appear in the captions of those figures. (b) The arithmetic average $\langle R_S\rangle$ and relative standard error $E_{R_S}\equiv \sqrt{\langle R_S^2\rangle-\langle R_S\rangle^2}/[\sqrt{N_M-1}\langle R_S\rangle]$ of $R_S(N,p_S)$, over all N_M samples with given values of p_S and N that had finite nonzero values of σ_e, were calculated and appear in Table I. Likewise, the arithmetic average $\langle R_I\rangle$ and relative standard error $E_{R_I}\equiv \sqrt{\langle R_I^2\rangle-\langle R_I\rangle^2}/[\sqrt{N_M-1}\langle R_I\rangle]$ of $R_I(N,p_I)$, over all N_M samples with given values of p_I and N that had finite nonzero values of σ_e, were calculated and appear in Table II.

Also exhibited in these tables are the average values and relative standard error of σ_e obtained from the same samples.

Clearly, the relative fluctuations of the ratios R_S, R_I are enormously reduced as compared to the relative fluctuations of the σ_e values. The errors quoted in the two tables for R_I and R_S are much smaller than the errors quoted in the captions of Figs. 9–12 for these two quantities: this is due to the fact that, in processing the figures, each of the plotted points is treated as a single exactly given datum and a least squares analysis is used to fit a straight line to those points. By contrast, in the two tables the conductance ratio of each pair of correlated samples is treated as a single exactly given datum and all those points are used to calculate an arithmetic average as well as the standard error. Clearly, the latter analysis has a

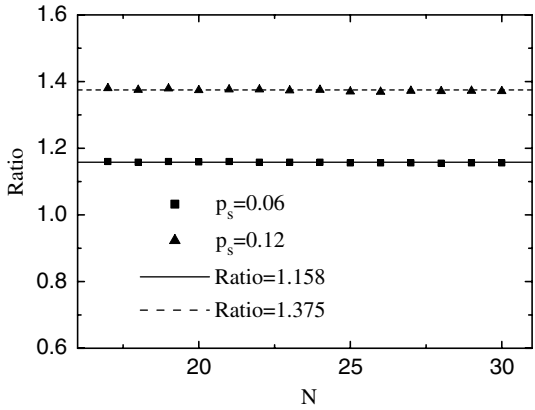

Fig. 9. Plot of the ratio R_S in 2D MS/I short random networks vs. the strip size N, at $p_M+p_S=p_c=0.5$ but with different fractions p_S. A least-squares fit to a straight line $R_S=aN+b$ leads to $a(p_S=0.06)=(-5.75\pm0.63)\times10^{-4}$, $b(p_S=0.06)=1.158\pm0.008$, $a(p_S=0.12)=(-1.59\pm0.13)\times10^{-3}$, $b(p_S=0.12)=1.375\pm0.009$.

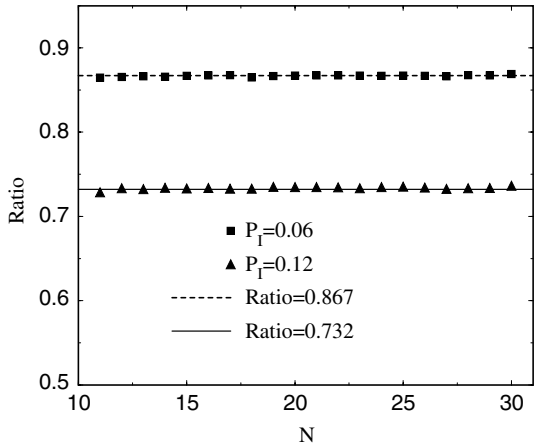

Fig. 10. Plot of the ratio R_I of 2D MI/S short random networks vs. the strip size N, at $p_S = p_c = 0.5$, with different fractions p_I. A least-squares fit to a straight line $R_I = aN + b$ leads to $a(p_I = 0.06) = (1.10 \pm 0.30) \times 10^{-4}$, $b(p_I = 0.06) = 0.867 \pm 0.009$, $a(p_I = 0.12) = (1.53 \pm 0.67) \times 10^{-4}$, $b(p_I = 0.12) = 0.732 \pm 0.008$.

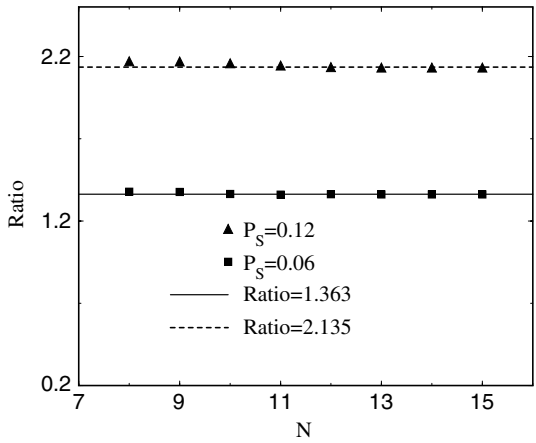

Fig. 11. Plot of the ratio R_S in 3D MS/I short random networks vs. the strip size N, at $p_M + p_S = p_c = 0.2492$ but with different fractions p_S. A least-squares fit to a straight line $R_S = aN + b$ leads to $a(p_S = 0.06) = (-2.35 \pm 0.74) \times 10^{-3}$, $b(p_S = 0.06) = 1.363 \pm 0.011$, $a(p_S = 0.12) = (-6.31 \pm 0.96) \times 10^{-4}$, $b(p_S = 0.12) = 2.135 \pm 0.015$.

much larger data base and can therefore lead to much smaller statistical errors *if all the data points are distributed around the same common average value*.

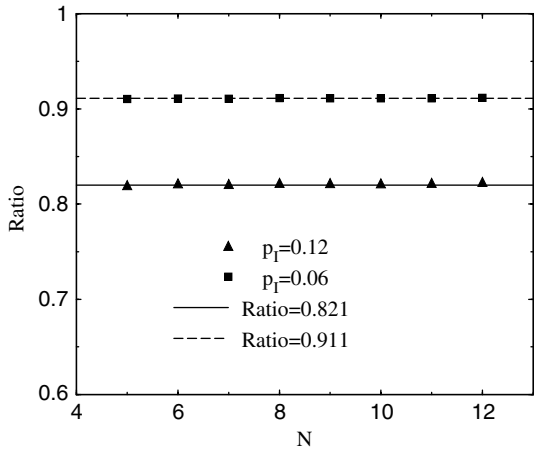

Fig. 12. Plot of the ratio R_I of 3D MI/S short random networks vs. the strip size N, at $p_S = p_c$=0.2492, with different fractions p_I. A least-squares fit to a straight line $R_I = aN + b$ leads to $a(p_I = 0.06) = (7.98 \pm 5.16) \times 10^{-5}$, $b(p_I = 0.06) = 0.911 \pm 0.008$, $a(p_I = 0.12) = (5.71 \pm 8.12) \times 10^{-5}$, $b(p_I = 0.12) = 0.821 \pm 0.007$.

The fact that the least-squares-fitted straight lines in Fig. 9 have a small negative slope whose magnitude increases with increasing p_S, still suggests a small tendency of t/ν to increase with p_S in 2D MS/I networks. However, in the 3D case (Fig. 11) the small negative slope seems first to increase when p_S is increased from 0 to 0.06, but then it decreases somewhat when p_S is further increased up to 0.12. Similarly, the small positive slopes in the least-squares-fitted straight lines of Figs. 10 and 12 still suggest that s/ν has a small tendency to increase when p_I is increased from 0 to 0.06 in the MI/S networks. However, it is not clear whether that tendency persists or is reversed when p_I is further increased up to 0.12.

The small nonzero slopes found in the almost horizontal fitted straight lines of Figs. 9–12 can easily be translated into approximate small changes in the critical exponents t/ν and s/ν. These changes turn out to be 1–2 orders of magnitude smaller than the systematic changes found in Section 3. Therefore, our conclusion from the improved method of analysis described in this section is that t/ν in the MS/I networks and s/ν in the MI/S networks are both unchanged from their values for the simple two-constituent M/I and M/S percolating networks, respectively.

5. CONCLUSIONS

A mixed-transfer-matrix algorithm was developed, which allows accurate computation of the macroscopic response of three-constituent $M/I/S$

Table I. *MS/I* Networks

2D						3D					
p_S	N	$\langle\sigma_e\rangle$	$E_{\sigma_e}(\%)$	$\langle R_S\rangle$	$E_{R_S}(\%)$	p_S	N	$\langle\sigma_e\rangle$	$E_{\sigma_e}(\%)$	$\langle R_S\rangle$	$E_{R_S}(\%)$
0.00	20	0.0304	0.6			0.00	8	0.0047	1.5		
	25	0.0238	0.5				10	0.0031	1.4		
	30	0.0200	0.4				12	0.0020	1.5		
0.06	20	0.0352	0.5	1.158	0.04	0.06	8	0.0065	1.5	1.378	0.1
	25	0.0276	0.5	1.157	0.08		10	0.0043	1.4	1.364	0.1
	30	0.0234	0.4	1.156	0.1		12	0.0028	1.4	1.362	0.2
0.12	20	0.0419	0.6	1.377	0.05		8	0.0106	1.6	2.221	0.2
	25	0.0328	0.7	1.372	0.08		10	0.0069	1.5	2.158	0.1
	30	0.0277	0.5	1.370	0.1		12	0.0045	1.5	2.135	0.1

Table II. *MI/S* Networks

2D						3D					
p_I	N	$\langle\sigma_e\rangle$	$E_{\sigma_e}(\%)$	$\langle R_I\rangle$	$E_{R_I}(\%)$	p_I	N	$\langle\sigma_e\rangle(\%)$	$E_{\sigma_e}(\%)$	$\langle R_I\rangle$	$E_{R_I}(\%)$
0.00	20	36.271	1.19			0.00	8	11.455	0.93		
	25	43.943	1.16				10	14.202	0.95		
	30	53.115	1.17				12	16.746	0.95		
0.06	20	31.269	1.12	0.8670	0.05	0.06	8	10.434	0.93	0.9119	0.01
	25	37.928	1.16	0.8671	0.06		10	12.934	0.95	0.9113	0.03
	30	46.000	1.17	0.8688	0.09		12	15.260	0.96	0.9117	0.03
0.12	20	26.279	1.21	0.7347	0.2	0.12	8	9.404	0.93	0.8232	0.05
	25	31.976	1.18	0.7352	0.15		10	11.665	0.95	0.8226	0.06
	30	38.768	1.19	0.7363	0.1		12	13.771	0.95	0.8233	0.06

conducting networks where the M bonds have finite conductance, while the I bonds have zero conductance, and the S bonds have infinite conductance. The algorithm was used to simulate random $M/I/S$ networks at the joint percolation threshold of the M and S constituents, as well as at the percolation threshold of the S constituent, in order to study the universality classes of those systems.

Our results provide strong empirical evidence that the universality assumptions which we set out to test are valid: MS/I networks at or near $p_I = 1 - p_c$ exhibit the same critical behavior for σ_e as do M/I networks.

Similarly, MI/S networks at or near $p_S = p_c$ exhibit the same critical behavior for σ_e as do M/S networks. These conclusions substantiate some of the crucial assumptions that had to be made when arguing for the existence of some nontrivial exact relations between critical behaviors of elastic and electrical properties of percolating systems. In particular, it follows from those assumptions that the elasticity critical exponents S and T of any macroscopic elastic stiffness modulus C_e satisfy $S = s$ and $T = t + 2\nu$, and that the three-constituent $M/I/S$ elastic percolating networks also lie in the same universality classes as the simple two-constituent M/I and M/S percolating elastic networks.

Other assumptions made in refs. 1 and 2, in the attempt to prove the exact relations $S = s$ and $T = t + 2\nu$, still remain to be verified. These include the assumption that the universality of critical behavior of C_e extends to the limit where, in the MS/I network, all the angle bending force constants for angles between bond pairs that are not FNB's are reset to be infinite, leaving only some of the FNB pairs with noninfinite force constants for the relative azimuth angle[2]. In 3D networks this means all the angles between nearest-neighbor bonds of types M and S become fixed. Another assumption is that, in M/I networks, the finite value of bond stretching constant k is an irrelevant parameter, and therefore the critical behavior of C_e is unchanged, as long as the total elastic energy of stretching all the bonds is less than the total energy of bending the azimuth angles between all the FNB pairs. This last assumption is required even to demonstrate that $S = s$ and $T = t + 2\nu$ in the case of 2D networks.

In contrast with the work reported in this article, the assumptions described in the preceding paragraph will need to be tested on percolating elastic networks, not on conducting networks.

The mixed-transfer-matrix approach presented here can also be applied to other network models where there are constituents whose physical parameters include finite values, as well as the values 0 and ∞. In particular, this approach can hopefully be applied to network models of high-field magneto-transport.

APPENDIX A: PROPERTIES OF THE MIXED MATRIX *D*

(a) Symmetry

$$D_{ij} = \begin{cases} D_{ji}, & \theta_i = \theta_j, \\ -D_{ji}, & \theta_i = -\theta_j. \end{cases}$$

As a consequence of this, the matrix $\theta_i D_{ij} \theta_j$ (note that summation is not implied in this expression!) is symmetric.

(b) Non-negativity

$$\sum_{ij} A_i D_{ij} A_j \geqslant 0$$

for any real values of the A_i.

APPENDIX B: ISOIATED SITE, SUPERCLUSTER, AND REPRESENTATIVE SITE

A terminal site (TS) J that is not connected by a conducting path to any other TS is called an "isolated site". We must then have $\theta_J = 1$ and $D_{Ji} = D_{iJ} = 0$ for any TS i, including J itself, i.e., $D_{JJ} = 0$.

If the TS $J_0, J_1, \ldots, J_{L-1}$ are connected to each other by perfectly conducting paths, then they are said to form a supercluster C_L. There are now two possible scenarios:

A: C_L is not connected by finite conductance paths to any other TS. In this case we choose $\theta_{J_0} = 1$, $\theta_{J_n} = -1$ $(n = 1, \ldots, L-1)$; then

$$\begin{aligned} D_{J_n J_0} &= 1, \\ D_{J_0 J_n} &= -1. \end{aligned} \tag{B.1}$$

All the other elements of D related to any TS of C_L are 0, including $D_{J_0 J_0} = 0$. Note that J_0 is chosen arbitrarily as a special TS in C_L—we call it the "representative site". The voltages of other TS in C_L are all equal to V_{J_0}.

B: C_L is connected to other TS by finite conducting paths. Such TS are called "normally connected terminal sites". In this case, two forms are possible for Θ and D:

(a) Similar to A, except that now $D_{J_0 J_0} > 0$ and $D_{J_0 i} \neq 0$, $D_{i J_0} \neq 0$ for any TS i that is normally connected to C_L.

(b) $\theta_{J_n} = -1$, $(n = 0, 1, \cdots, L-1)$: In this case the supercluster TS are all equivalent and there is no special representative site. The elements of D that involve any one or two terminal sites in C_L are all equal and positive. Elements of D that involve any TS in C_L and a particular normally connected TS outside C_L all have the same nonzero real value which is determined by that particular site.

We only use the form (a) in our calculation. In that case, if $D_{kk} = 0$ and $\theta_k = -1$, we know that the TS k is in a supercluster. On the other hand, if $D_{kk} = 0$ and $\theta_k = 1$, then we know that k is either an isolated site

or a representative site. In order to decide in this last case what is the character of the TS k, we use the following criterion:

$$\sum_{i=1}^{m} D_{ik} = 0, \quad \Rightarrow k \text{ is an isolated site,}$$
$$\sum_{i=1}^{m} D_{ik} = L, \quad \Rightarrow k \text{ is a representative site in a supercluster } C_L \text{ with } L \text{ TS.}$$

In addition, we know that $i \in C_L$ if $D_{ik} = 1$, and that $i \notin C_L$ if $D_{ik} = 0$. If we used the form (b), or allowed both of the forms (a) and (b) to be used, then it would be difficult to identify the character of TS k when $D_{kk} = 0$: we would need to check all the $m \times m$ elements of D, and the computation would become hopelessly complex and time consuming. That is why we only use the form (a) in our calculations: after a bond is added, we check the elements of the vector Θ and the diagonal elements of the matrix D. If $\theta_k = -1$, and $D_{kk} \neq 0$, we switch the value of θ_k to $\theta_k = 1$, and D is updated as follows:

$$\begin{aligned} &D'_{kk} = 1/D_{kk}, \\ &D'_{ik} = D_{ik}/D_{kk}, && i = 1, \ldots, m \quad (i \neq k), \\ &D'_{kj} = -D_{kj}/D_{kk}, && j = 1, \ldots, m \quad (j \neq k), \\ &D'_{ij} = D_{ij} - D_{kj}/D_{kk}, && i, j = 1, \ldots, m \quad (i, j \neq k). \end{aligned} \tag{B.2}$$

This has the effect of changing the form (b) to the form (a). It is useful to note that any current that is induced to flow into a supercluster C_L (i.e., any current which is not directly applied to it) can only flow into the representative TS of C_L. Also, a negative value of $\theta_i = -1$ only appears if i is a non-representative TS of some supercluster. All other TS have $\theta_i = 1$.

APPENDIX C: OBTAINING THE MACROSCOPIC CONDUCTANCE OF A STRIP SAMPLE

We note that, for a TS that is not in a supercluster, we must have $\theta_k = 1$. Therefore, if $\theta_k = -1$, then the TS k must belong to a supercluster. Because we use the form (a), there is then always one TS in the supercluster whose characteristic element of the vector Θ equals 1. Since we maintain $\theta_1 = 1$ throughout the construction of the strip, therefore at the end of the calculation, after we add insulating x-bonds at the TS i ($i = 2, \ldots, m-1$), we will have one of the following two situations: (a) $\theta_m = 1$

and $D_{11} = D_{mm} = -D_{1m} = -D_{m1}$, in which case D_{11} is the noninfinite conductance of the short strip, while the other elements of D all vanish. (b) $\theta_m = -1$ and the TS m is in a supercluster together with the TS 1: the strip then has an infinite conductance.

APPENDIX D: THE UPDATING ALGORITHM

Based on the properties of matrix D and supercluster, we describe the algorithm for updating the matrix D and the characteristic vector Θ every time that a bond is added to the strip network. In this section, D_{ij} and θ_i denote elements of the old D and Θ, while D'_{ij} and θ'_i denote elements of the updated matrix D' and characteristic vector Θ'. We use a Greek subscript α to denote the site where an x-bond is added. That site ceases to be a TS, but a new TS now appears at the other end of the added x-bond. This new TS is also denoted by α. y-bonds and z-bonds are added between two adjacent sites which are denoted by α and β. Unless stated otherwise, the indices i and j range from 1 up to m. g is the conductance of a normal bond.

Adding an x-bond at site α

(1) Normal bond, $\theta_\alpha = 1$:

$$\begin{aligned} D'_{ij} &= D_{ij} - \frac{D_{i\alpha} D_{\alpha j}}{g + D_{\alpha\alpha}}, \\ \theta'_i &= \theta_i . \end{aligned} \tag{D.1}$$

(2) Normal bond, $\theta_\alpha = -1$:

$$\begin{aligned} D'_{ij} &= D_{ij} + \frac{1}{g}\delta_{i\alpha}\delta_{j\alpha}, \\ \theta'_i &= \theta_i . \end{aligned} \tag{D.2}$$

(3) Perfectly insulating bond, $\theta_\alpha = 1$: the new site α is an isolated site. The following cases are possible:

a. $D_{\alpha\alpha} \neq 0$:

$$\begin{aligned} D'_{ij} &= D_{ij} - \frac{D_{i\alpha} D_{\alpha j}}{D_{\alpha\alpha}}, \\ \theta'_i &= \theta_i . \end{aligned} \tag{D.3}$$

b. $D_{\alpha\alpha} = 0$; there are now two possibilities:

(i) $D_{\alpha j}=0$ for all values of j: the old site α was not connected to any other site, thus nothing is changed after adding a perfectly insulating x-bond, therefore no changes are made in D or Θ. In particular, we have, for any i, j,

$$\begin{aligned} &D'_{i\alpha}=D'_{\alpha j}=0,\\ &\theta'_i=\theta_i. \end{aligned} \tag{D.4}$$

(ii) $D_{\alpha J_n}=-1 (n=1,\ldots,L-1)$: the old site α was a representative site in a supercluster C_L. If $L=2$, that cluster becomes two isolated sites after adding a perfectly insulating x-bond at α, therefore, for any i, j, we have

$$\begin{aligned} &D'_{i\alpha}=D'_{\alpha j}=D'_{iJ_1}=D'_{J_1 j}=0,\\ &\theta'_{J_1}=1. \end{aligned} \tag{D.5}$$

All the other elements in D and Θ remain unchanged.

If $L>2$, there will be no representative site in the remaining supercluster C_{L-1}, therefore we must choose one of the TS in C_{L-1} as the new representative site J_1. Keeping in mind that the new site α is an isolated site, we get, for any i, j,

$$\begin{aligned} &D'_{i\alpha}=D'_{\alpha j}=0,\\ &D'_{J_n J_1}=-D'_{J_1 J_n}=1, \quad (n=2,\ldots,L-1),\\ &\theta'_{J_1}=1. \end{aligned} \tag{D.6}$$

All the other elements in D and Θ are unchanged.

(4) Perfectly insulating bond, $\theta_\alpha=-1$: in this case site α is in a supercluster C_L, But because it is not a representative site, we only need to reset the elements of D and Θ which include the index α. All the other elements remain unchanged. Thus, for any i, j, we have

$$\begin{aligned} &D'_{i\alpha}=D'_{\alpha j}=0,\\ &\theta'_\alpha=1. \end{aligned} \tag{D.7}$$

This procedure remains valid even when $L=2$, i.e., for a two-sites supercluster C_2.

(5) Perfectly conducting bond: D and Θ remain unchanged.

Adding a vertical bond (z-bond or y-bond) between α and β

(1) Normal bond, $\theta_\alpha = 1$, $\theta_\beta = 1$:

$$\begin{aligned} D'_{ij} &= D_{ij} + g(\delta_{\alpha j} - \delta_{\beta j})(\delta_{\alpha i} - \delta_{\beta i}), \\ \theta'_i &= \theta_i . \end{aligned} \tag{D.8}$$

(2) Normal bond, $\theta_\alpha = -1$, $\theta_\beta = -1$:

$$\begin{aligned} D'_{ij} &= D_{ij} - \frac{g(D_{i\alpha} - D_{i\beta})(D_{\alpha j} - D_{\beta j})}{1 + g(D_{\alpha\alpha} + D_{\beta\beta} - D_{\alpha\beta} - D_{\beta\alpha})}, \\ \theta'_i &= \theta_i . \end{aligned} \tag{D.9}$$

(3) Normal bond, $\theta_\alpha = 1$, $\theta_\beta = -1$;

$$\begin{aligned} D'_{ij} &= D_{ij} - g\frac{D_{i\beta}D_{\beta j} - D_{i\beta}\delta_{j\alpha} + D_{\beta j}\delta_{i\alpha} - \delta_{i\alpha}\delta_{j\alpha}}{1 + g D_{\beta\beta}}, \\ \theta'_i &= \theta_i . \end{aligned} \tag{D.10}$$

(4) Perfectly conducting bond, $\theta_\alpha = 1$, $\theta_\beta = 1$: α and β become a two-site supercluster C_2. Thus, one of the two characteristic vector elements should switch its value to -1. Since we want to keep $\theta_1 \equiv 1$ always, the TS with the larger index is the one whose characteristic vector element should be switched. Supposing $\beta > \alpha$, we get

$$\begin{aligned} D'_{\alpha\alpha} &= D_{\alpha\alpha} + D_{\beta\beta} + D_{\alpha\beta} + D_{\beta\alpha}, & \\ D'_{\alpha\beta} &= -1, & \\ D'_{\beta\alpha} &= 1, & \\ D'_{\alpha j} &= D_{\alpha j} + D_{\beta j}, & j \neq \alpha, \beta, \\ D'_{i,\alpha} &= D_{i\alpha} + D_{i\beta}, & i \neq \alpha, \beta, \\ D'_{\beta j} &= D_{i\beta} = 0, & i, j \neq \alpha, \\ D'_{ij} &= D_{i,j}, & i, j \neq \alpha, \beta, \\ \theta'_\beta &= -1, & \\ \theta'_i &= \theta_i, & i \neq \beta. \end{aligned} \tag{D.11}$$

(5) Perfectly conducting bond, $\theta_\alpha = -1$, $\theta_\beta = -1$: because we use the form (a), both site α and site β are in superclusters, possibly even in the same supercluster. Two representative sites of two clusters can be found using Eq. (B.1). We then connect the two representative sites, transforming D and Θ according to Eq. (D.11): physically this is equivalent to adding a perfectly conducting bond between α and β. If the two representative sites

are the same site, then α and β were in the same supercluster even before addition of the perfectly conducting bond between them. In that case D and Θ remain unchanged.

(6) Perfectly conducting bond, $\theta_\alpha = 1$, $\theta_\beta = -1$: suppose that site β is in a supercluster C_L. If $D_{\beta\alpha} = D_{\alpha\beta} = 1$, then α is the representative site of C_L, therefore nothing is changed. If $\alpha \neq 1$ and $D_{\alpha\beta} = D_{\beta\alpha} = 0$, then α will become a nonrepresentative site of C_L after adding the perfectly conducting bond. We thus get

$$\begin{aligned}
&D'_{\alpha\alpha} = D'_{\beta\beta} = D'_{\alpha\beta} = D'_{\beta\alpha} = 0, \\
&D'_{\alpha j} = D'_{\beta j} = D_{\beta j}, && (j \neq \alpha, \beta), \\
&D'_{i\alpha} = D'_{i\beta} = D_{i\beta}, && (i \neq \alpha, \beta), \\
&D'_{ij} = D_{i,j} + D_{i\alpha} D_{\beta j} - D_{i\beta} D_{\alpha j} - D_{\alpha\alpha} D_{i\beta} D_{\beta j}, && (i, j \neq \alpha, \beta), \\
&\theta'_\alpha = -1, \\
&\theta'_i = \theta_i, && (i \neq \alpha).
\end{aligned} \tag{D.12}$$

If $\alpha = 1$ and $D_{\alpha\beta} = D_{\beta\alpha} = 0$, its characteristic vector element must be $\theta_1 = 1 \neq -1$. We must then first find the representative site of C_L, then, using Eq. (D.11), we connect it to α by a perfectly conducting bond. This is physically equivalent to actually connecting the TS α and β by such a bond. The TS α then becomes the new representative TS of the expanded supercluster.

(7) Perfectly insulating bond: D and Θ remain unchanged.

ACKNOWLEDGMENTS

This research was supported, in part, by grants from the US-Israel Bi-national Science Foundation and the Israel Science Foundation. Partial support for the work of XL was provided by the Sackler Institute for Solid State Physics of Tel Aviv University.

REFERENCES

1. D. J. Bergman, *Phys. Rev. E* **65**:154202 (2002).
2. D. J. Bergman, *J. Stat. Phys.* **111**:171 (2002).
3. Y. Kantor and I. Webman, *Phys. Rev. Lett.* **52**:1891 (1984).
4. A. Aharony and D. Stauffer, *Introduction to Percolation Theory*, 2nd edition, Taylor and Francis, London, 1992.
5. B. Derrida, J. G. Zabolitzky, J. Vannimenus, and D. Stauffer, *J. Stat. Phys.* **36**:31 (1984).
6. H. J. Herrmann and B. Derrida, *Phys. Rev. B* **30**:4080 (1984).
7. B. Derrida and J. Vannimenus, *J. Phys. A* **15**:L557 (1982).
8. D. J. Bergman, *Phys. Rev. B* **33**: 2013 (1986).